Cusp properties of high harmonic loops

Despoina Pazouli,[*] Anastasios Avgoustidis,[†] and Edmund J. Copeland[‡]
School of Physics and Astronomy, University of Nottingham, Nottingham NG7 2RD, United Kingdom

(Received 16 November 2020; accepted 25 February 2021; published 29 March 2021)

In determining the gravitational signal of cusps from a network of cosmic string loops, a number of key parameters have to be assumed. These include the typical number of cusps per period of string oscillation and the typical values of the sharpness parameters of left- and right-moving waves on the string, evaluated at the cusp event. Both of these are important, as the power stored in the gravitational waves emitted from the loops of string is proportional to the number of cusps per period and inversely proportional to the product of the sharpness parameters associated with the left- and right-moving modes on the string. In suitable units, both of these quantities are usually thought to be of order unity. To try and place these parameters on a more robust footing, we analyze in detail a large number of randomly chosen loops of string that can have high harmonics associated with them, such as one might expect to form by chopping off an infinite string in the early Universe. This allows us to analyze tens of thousands of loops and obtain detailed statistics on these crucial parameters. While we find in general the sharpness parameters are indeed close to unity, as assumed in previous work [with occasional exceptions where they can become $O(10^{-2})$], the cusp number per period scales directly with the number of harmonics on the loop and can be significantly larger than unity. This opens up the possibility of larger signals than would have otherwise been expected, potentially leading to tighter bounds on the dimensionless cosmic string tension $G\mu$.

DOI: 10.1103/PhysRevD.103.063536

I. INTRODUCTION

Cosmic strings are linelike topological defects produced by symmetry breaking phase transitions in a wide range of early Universe models [1–6]. They form tangles or networks that evolve dynamically and can produce a host of potentially observable signals. In particular, they are active, incoherent sources of cosmological perturbations, and so their predicted effects on the cosmic microwave background (CMB) are very different from those of passive, coherent perturbations generated by cosmic inflation [7–11]. This has allowed cosmic strings to be strongly constrained, having a maximum allowed contribution to the CMB anisotropy at the level of approximately 1% [12,13].

While cosmic strings have been ruled out as the main source of the observed CMB anisotropy, they remain an important subject in modern cosmology. Indeed, the formation of string networks is a generic prediction in a wide range of models of the early Universe [14–21], and so they are extremely interesting from a theoretical point of view. At the same time, they have a rich phenomenology with observational signals relevant to several areas of cosmology and astrophysics [6]. Thus, cosmic strings open an exciting observational window into the early Universe. Their observation would be a major discovery in physics, and as a bonus, it would also provide important quantitative information about the physics of the early Universe (e.g., the energy scale of the symmetry breaking phase transition that produced the string network). On the other hand, even failure to observe strings is of significant scientific value; as observational sensitivity improves and bounds on cosmic strings become tighter, we are excluding more of the parameter space of our models of the early Universe.

The discovery of gravitational waves has reinforced interest in the physics of cosmic strings. The evolution of string networks leads to the production of closed string loops, which decay via gravitational wave emission. At this point, we should acknowledge this is not a uniformly accepted outcome for the string decay. Being modeled as Abelian-Higgs strings, there are also claims in the literature that the dominant form of decay is via the fields themselves and not gravitationally [22]. This is an important issue; for recent work considering the relative importance of both contributions, see Refs. [23,24]. We will be considering the case where the primary decay channel is through gravitational radiation, giving rise to a stochastic background of gravitational waves. Most of the emission comes from specific

[*]Despoina.Pazouli@nottingham.ac.uk
[†]Anastasios.Avgoustidis@nottingham.ac.uk
[‡]Edmund.Copeland@nottingham.ac.uk

events on the string, known as cusps, arising when the local velocity of the string momentarily hits the speed of light, thus producing a burst of beamed gravitational radiation. Kinks, points on the string where the tangent to the string is discontinuous, are also known to contribute significantly to the gravitational wave signal. These signals are now being targeted by gravitational wave detectors including LIGO [25–27] and LISA [28,29]. Such targeting brings with it the need for a better quantitative understanding of gravitational radiation from string networks. Some of the most stringent observational bounds on cosmic strings come from their predicted stochastic gravitational wave background, which can be constrained either indirectly through pulsar timing observations [30–34] or directly by gravitational wave detectors [26]. However, these constraints are also the most sensitive to largely unknown parameters, like, for example, the typical size of string loops in the network. Indeed, while the evolution of the long string component of the network is well understood, the quantitative modeling of the loop component remains uncertain. In particular, the typical size of loops depends on the loop production function [2] (the number density of loops as a function of loop size and time), which has been the subject of active debate in recent years [22,35–43].

At present, there are three models used for deriving constraints and forecasts on string networks based on their stochastic gravitational wave background. These models, referred to as models 1/I, 2/II, and 3/III in Refs. [27,29], respectively, differ significantly in their assumed/derived loop distribution functions. As we are entering this exciting era of direct gravitational wave detection, it is imperative that as the modeling be improved the associated loop parameters become better quantified. In this paper, we focus on two key parameters, the number of string cusps per oscillation period and the sharpness of cusps, both of which are important components of the overall gravitational signal from cusps. While there has been a considerable amount of work on the role of cusps on networks of cosmic string loops (see, for example, Refs. [29,41,42,44–53]), the distribution of cusps on higher harmonic loops has not to date been studied in detail. An early attempt to address the issue can be found in the work by Copi and Vachaspati [54], who used numerical simulations to characterize attractor non-self-intersecting loop shapes, studying their length, velocity, kink, and cusp distributions. To reach that stage, they began with initial loops containing M higher harmonic modes and argued that such loops have on average M^2 cusps. They also discovered that on average large loops will split into $3M$ stable loops within two oscillation periods (independently of M), with the stable loops being described by a degenerate kinky loop, coplanar and rectangular. These final loops were found to have a 40% chance of containing a cusp.

In reality, we do not really know the harmonic distribution at formation of cosmic string loops, but we do know there could be loops formed off the long string network or as individual loops in the early Universe that have many harmonics on them. The traditional picture of such loops is that as they evolve the majority of them undergo a period where they self-intersect. The initial loop then breaks into two daughter loops, with the accompanying formation of a pair of kinks on each daughter loop. These may well then self-intersect, and a cascade process takes place, whereby the initial high harmonic loop ends up in a class of much smaller non-self-intersecting loops [55–57]. The effect of the fragmentation process on the gravitational wave production of the network is studied in Refs. [58,59]. The cusps associated with such non-self-intersecting loops play an important role through the strong beams of high-frequency gravitational waves they produce, which leads to a stringy non-Gaussian distribution in the stochastic ensemble of gravitational waves generated by a cosmological network of oscillating loops, and also, crucially, occasional sharp bursts of gravitational waves from the cusp regions that stand out above the confusion of gravitational wave noise made by smaller overlapping bursts. The results of Damour and Vilenkin [52] suggest that if only 10% of all string loops have cusps the gravitational wave bursts would be detectable by Advanced LIGO or LISA for string tensions μ down below $G\mu \sim 10^{-13}$, where G is Newton's constant.

In determining these constraints, there are two important parameters whose values need to be assumed. Given the spacetime position of a string $X_\mu(\sigma,\tau)$, where σ, τ are the worldsheet coordinates of the string, as we will shortly see, the general solution for the string is given in terms of right- and left-moving modes traveling along it, $\vec{a}(u)$ and $\vec{b}(v)$, where $u=\sigma-\tau$ and $v=\sigma+\tau$. Now, two key parameters involved in the gravitational wave calculation are the second derivative of the string position evaluated at the cusp $\partial_t^2 X$ (a measure of "cusp sharpness") and the average number of cusps formed per loop period $T_\ell=\ell/2$, where ℓ is the invariant length of the loop. In Eq. (3.21) of Ref. [52], the authors argue that the generic order of magnitude estimate for $|\vec{a}''|\sim 2\pi/\ell \sim |\vec{b}''|$, where $\vec{a}''\equiv\frac{d^2\vec{a}}{du^2}$ and $\vec{b}''\equiv\frac{d^2\vec{b}}{dv^2}$ evaluated at the cusp. In other words, they expect the coefficient to be of order unity ($2\pi/\ell$ is the natural unit for a string loop). In terms of the number of cusps per loop oscillation, quantified by parameter c in Eq. (5.14) of Ref. [52], the authors consider typical values of $c\sim 1$. This parameter is meant to account for the possibility that all of the loops have of order one cusp per oscillation ($c\sim 1$) or, for example, only 10% of the loops have a cusp on them per oscillation ($c\sim 0.1$). As shown in Fig. 1 of Ref. [52], c can have a significant impact on the strength of the gravitational wave amplitude of bursts emitted by cosmic string cusps. Similarly, knowing the true range of values of $|\vec{a}''|$ and $|\vec{b}''|$ is also important for a proper estimate of the strength of the signal emerging from cusp bursts. This is clear from Eqs. (3.11), (3.12), and (3.23) of Ref. [52], in which the logarithmic Fourier

transform of the gravitational wave burst asymptotic waveform for the cusp emission, and hence the amplitude of the wave arriving on Earth, depends on terms of the form $1/(|\vec{a}''||\vec{b}''|)^{1/3}$. In particular, if it turns out that a significant fraction of the cusps had associated values $|\vec{a}''| \ll 1$ and $|\vec{b}''| \ll 1$ (in units of $2\pi/\ell$), then it could lead to a significant enhancement of the strength of the signal produced.

It is apparent from the above discussion that to accurately quantify gravitational radiation from string networks one must understand (a) how these two parameters (number of cusps per oscillation period and cusp sharpness) behave as functions of the loop harmonic number and (b) what is the expected loop distribution in terms of their harmonic content or, at the very least, what is the harmonic content of a typical loop in the network. Here, we focus on a, considering the behavior of individual loops in isolation, without examining the typicality of the loop in the network (we will present our results on b in a forthcoming publication [60]). A key goal of this work is to analyze these two parameters for a wide range of high harmonic loops to establish whether there is a correlation between the number of cusps and the harmonic order of the loop and what range/distribution of values we have for the magnitude of $|\vec{a}''|$ and $|\vec{b}''|$ evaluated at the cusps. For concreteness, we work with the odd-harmonic string [61,62], a family of cosmic string solutions which can be expressed in analytic form to arbitrarily high harmonics. In the following, we will use the convention that spacetime indices are in greek, taking the values $\mu = 0, 1, 2, 3$, while space indices are in latin taking the values $i = 1, 2, 3$.

This paper is organized as follows. In Sec. II, we review the basics of the Nambu-Goto approach to string modeling, while in Sec. III, we review the odd-harmonic string solutions, which are the focus of this work. In Sec. IV, we generate large ensembles of odd-harmonic string solutions and study their cusp number and sharpness distributions. We conclude in Sec. V.

II. NAMBU-GOTO STRING

In this section, we will give a brief introduction to the dynamics of Nambu-Goto strings in flat spacetime—more details can be found, for example, in the classic textbooks of Vilenkin and Shellard [2] and Zwiebach [63].

The background spacetime where the string moves is assumed to be a smooth four-dimensional Lorentzian manifold with a metric $g_{\mu\nu}$, and each point on the manifold is identified by the spacetime coordinates $x^\mu = (x^0, x^1, x^2, x^3)$. We model the closed string dynamics using the Nambu-Goto action. In this approach, the string is a one-dimensional object, and its world history can be represented by a two-dimensional surface in spacetime, the worldsheet. The mapping functions

$$X^\mu = X^\mu(\tau, \sigma) \tag{2.1}$$

map the worldsheet parameters (τ, σ), used to parametrize the two-dimensional surface, to the spacetime coordinates x^μ. The parameter σ describes different points on the string on, and it is subject to periodic identification, since we assume a closed string, while τ is the time parameter on the worldsheet. The induced metric, i.e., the metric induced on the worldsheet from the spacetime metric $g_{\mu\nu}$, is

$$\gamma_{AB} = g_{\mu\nu} \frac{\partial X^\mu}{\partial \xi^A} \frac{\partial X^\nu}{\partial \xi^B}. \tag{2.2}$$

The indices A and B take values from 0 to 1, and $\xi^0 = \tau, \xi^1 = \sigma$. The Nambu-Goto action is proportional to the surface area swept out by the string in spacetime

$$S = -\mu \int d\tau \oint d\sigma \sqrt{-\det \gamma}, \tag{2.3}$$

where μ is the string tension and $\det \gamma$ is the determinant of the induced metric γ_{AB}.

Restricting our analysis to a cosmic string living in a flat spacetime, the spacetime metric becomes $g_{\mu\nu} = \eta_{\mu\nu} = \mathrm{diag}(-1, 1, 1, 1)$. By varying the action (2.3) with respect to the mapping functions X^μ, we obtain the equations of motion for the string in flat spacetime,

$$\partial_A(\sqrt{-\det \gamma}\gamma^{AB}\partial_B x^\mu) = 0, \tag{2.4}$$

where $\partial_A = \partial/\partial\xi^A$. Since the action is invariant under arbitrary reparametrizations of the worldsheet, we are free to impose two conditions on the worldsheet parameters, thereby fixing the gauge. It is convenient to choose the conformal gauge $\gamma_{AB} = \sqrt{-\det \gamma}\eta_{AB}$, where $\eta_{AB} = \mathrm{diag}(-1, 1)$, the two-dimensional Minkowski metric. The conformal gauge imposes the Virasoro constraints

$$\eta_{\mu\nu} \frac{\partial X^\mu}{\partial \tau} \frac{\partial X^\nu}{\partial \sigma} = 0, \tag{2.5}$$

$$\eta_{\mu\nu} \frac{\partial X^\mu}{\partial \tau} \frac{\partial X^\nu}{\partial \tau} + \eta_{\mu\nu} \frac{\partial X^\mu}{\partial \sigma} \frac{\partial X^\nu}{\partial \sigma} = 0. \tag{2.6}$$

Equation (2.4) is then simplified to a two-dimensional wave equation of motion for the string in flat spacetime,

$$\left(\frac{\partial^2}{\partial \sigma^2} - \frac{\partial^2}{\partial \tau^2}\right) X^\mu(\tau, \sigma) = 0, \tag{2.7}$$

constrained by the Virasoro conditions. The general solution of the Nambu-Goto equations of motion in the conformal gauge is therefore a superposition of a left-moving and a right-moving waveforms. Notice that a

solution to (2.7) for $\mu = 0$ is $X^0 = \tau$, which we can choose to fix the remaining gauge invariance. Note that our gauge choices have fixed the possible reparametrizations of the worldsheet parameters, apart from a constant shift in σ. We can now write the general solution of the string motion as

$$X^0 = \tau, \quad X^i(\tau,\sigma) = \frac{1}{2}(a^i(u) + b^i(v)), \tag{2.8}$$

constrained by

$$\eta_{ij}\frac{da^i}{du}\frac{da^j}{du} = 1, \qquad \eta_{ij}\frac{db^i}{dv}\frac{db^j}{dv} = 1. \tag{2.9}$$

To reiterate, in the above, we have defined $u = \sigma - \tau$ and $v = \sigma + \tau$, and $\vec{a}(u)$ and $\vec{b}(v)$ are the right- and left-moving vector mode functions, respectively. Using the notation $r'(u) = dr/du$, etc., and $\vec{a}^2 = \eta_{ij}a^i a^j$, the Virasoro conditions are then written simply as

$$\vec{a}'^2 = \vec{b}'^2 = 1; \tag{2.10}$$

that is, the functions $\vec{a}'(u)$ and $\vec{b}'(v)$ both have constant unit magnitude. Therefore, they trace closed curves on a unit 2-sphere, which is called the Kibble-Turok sphere. Note that up to this point we assumed that γ_{AB} is nondegenerate. However, there are singular points on the worldsheet where $\det\gamma$ becomes zero. The velocity of the string momentarily reaches the speed of light at these points, which are called cusps. Another type of singular points on the worldsheet are the kinks, which occur where the derivatives of the right- and left-movers have discontinuities. These points, namely, the cusps and kinks, play an important role in the evolution of the string since the gravitational radiation they emit dominates the gravitational wave signal from the string.

We will choose for convenience the period in σ to be 2π. Since the loop is closed, the string trajectory should satisfy that $X^\mu(\tau,\sigma+2\pi) = X^\mu(\tau,\sigma)$. It can then be shown that $a^\mu(u) - a^\mu(u+2\pi) = -b^\mu(v) + b^\mu(v+2\pi)$ and also that the string trajectory $X^\mu(\tau,\sigma)$ has effective period π, since $X^\mu(\tau+\pi,\sigma+\pi) = X^\mu(\tau,\sigma)$. This is the cosmic string fundamental oscillation period $T_1 = \pi$. For specific families of cosmic string solutions, it is possible for the period to be less than T_1, for example, when the string trajectory is invariant under a translation of a fraction of π, such as the case with a nonplanar single harmonic loop [64]. In the center-of-mass frame, the functions $\vec{a}'(u)$ and $\vec{b}'(v)$ should satisfy the conditions

$$\int_0^{2\pi}\vec{a}'du = \int_0^{2\pi}\vec{b}'dv = 0. \tag{2.11}$$

Therefore, in the center-of-mass frame, the functions $\vec{a}(u)$ and $\vec{b}(v)$ have period 2π, and so do $\vec{a}'(u)$ and $\vec{b}'(v)$.

III. ODD-HARMONIC STRING

The general solution of the cosmic string loop equations of motion can be expanded as a Fourier series. In our study, we will require solutions of equations that involve the derivatives of the left- and right-movers, $\vec{a}'(u)$ and $\vec{b}'(v)$. For that reason, we will parametrize these quantities hereafter, instead of the loop trajectory. The Fourier series expansions of $a'(u)$ and $b'(v)$ are written as

$$\vec{a}'_N(u) = \vec{V} + \sum_{n=1}^{N}\vec{A}_n\cos(nu) + \sum_{n=1}^{N}\vec{B}_n\sin(nu), \tag{3.1}$$

$$\vec{b}'_M(v) = -\vec{V} + \sum_{n=1}^{M}\vec{C}_n\cos(nv) + \sum_{n=1}^{M}\vec{D}_n\sin(nv), \tag{3.2}$$

where $N, M \in \mathbb{N}$ correspond to the harmonic order of the string movers [2]. The constant terms of $\vec{a}'_N(u)$ and of $\vec{b}'_M(v)$ are constrained to be opposite to each other due to the periodicity of the loops. The solutions (3.1) and (3.2) must satisfy the Virasoro conditions (2.9), which impose a nonlinear set of conditions on the vector coefficients, $\vec{A}_n$, $\vec{B}_n$, $\vec{C}_n$, $\vec{D}_n$, and $\vec{V}$. A method to solve these conditions was introduced by Brown *et al.*, who used a product representation method (and its corresponding spinorial representation) allowing them to describe the loop trajectory in terms of a matrix product [61,62]. Introducing $\vec{h}'_N(u)$ to represent either the derivatives of the left- $[\vec{a}'(u)]$ or right-moving $[\vec{b}'(v)]$ modes of a string with N harmonic modes, they can be written in the functional form

$$\vec{h}'_N(u) = \rho_{N+1}R_z(u)\ldots\rho_3 R_z(u)\rho_2 R_z(u)\rho_1\vec{k}, \tag{3.3}$$

where

$$\rho_i = \rho(\theta_i,\phi_i) = R_z(-\theta_i)R_x(\phi_i)R_z(\theta_i), \tag{3.4}$$

such that

$$0 \le \phi_i \le 2\pi, \qquad 0 \le \theta_i \le \pi \qquad i = 1,\ldots,N+1 \tag{3.5}$$

and

$$R_z(\omega) = \begin{pmatrix}\cos\omega & -\sin\omega & 0\\ \sin\omega & \cos\omega & 0\\ 0 & 0 & 1\end{pmatrix}, \tag{3.6}$$

$$R_x(\omega) = \begin{pmatrix}1 & 0 & 0\\ 0 & \cos\omega & -\sin\omega\\ 0 & \sin\omega & \cos\omega\end{pmatrix}. \tag{3.7}$$

Note that we have assumed a three-dimensional Cartesian coordinate system xyz, with unit vectors $(\vec{i},\vec{j},\vec{k})$. We have

introduced a matrix notation, where $R_x(\phi)$ denotes a rotation of angle ϕ around the x axis. In expression (3.3), we chose the $\vec{k}$ unit vector, without loss of generality; any other unit vector can be chosen, and the same rule can be applied, or equivalently we can change the coordinate system alignment.

The product representation method provides a general expression for the cosmic string solution up to any finite order of harmonics as a product of matrices. However, if we wish to describe the string in its center-of-mass frame, then the cosmic string solution must also satisfy the condition (2.11), which implies that both $\vec{a}'(u)$ and $\vec{b}'(v)$ have period 2π. Although a general solution for any order N that solves (2.11) has not been found analytically, strings comprising only odd harmonics are in fact a solution as originally shown by Siemens and Kibble [65]. This loss of generality is the small price we have to pay in order to move to the center-of-mass frame of the cosmic string. By applying Eq. (3.3) to the case where all harmonics on the N harmonic string are odd, we obtain

$$\vec{h}'_N(u) = \rho_{N+2} R_z(2u) \rho_N R_z(2u) \ldots R_z(2u) \rho_3 R_z(u) \rho_1 \vec{k}, \tag{3.8}$$

with $\theta_1 = -\pi/2$ and $\phi_1 = \pi/2$ for both $\vec{a}'$ and $\vec{b}'$. As we have mentioned, a key goal of ours in this work is to determine the number of cusps produced per period on an odd-harmonic cosmic string, the relative positions of the points where the cusps occur, and the magnitude of the second derivatives of the left- and right-movers evaluated at the cusps. Given that these quantities are invariant under orientations of the string in the plane, we can further simplify our solution, while making sure that the relative orientation freedom of $\vec{a}'(u)$ and $\vec{b}'(v)$ is preserved. Therefore, we are free to eliminate parameters from the orientation freedom of the string by removing the θ_{N+2} parameter from $a'(u)$ and the θ_{M+2} and ϕ_{M+2} parameters from $b'(v)$. Leaving the parameter ϕ_{N+2} in $a(u)$ ensures the relative freedom of the string movers [62,65]. The solutions for the derivatives of the right- and left-movers that we obtain are

$$\vec{a}'_N(u) = R_x(\phi_{N+2}) R_z(2u) \rho_N R_z(2u) \ldots R_z(2u) \rho_3 R_z(u) \vec{i} \tag{3.9}$$

and

$$\vec{b}'_M(v) = R_z(2v) \rho_M R_z(2v) \ldots R_z(2v) \rho_3 R_z(v) \vec{i}, \tag{3.10}$$

respectively. We will call the string appearing in Eqs. (3.9) and (3.10) the N/M odd harmonic string, referring to the harmonic order we have chosen for $a'(u)$ and $b'(v)$, respectively. In our study, we will use this parametrization of cosmic string loops to obtain our key results. The angles that appear in the matrix $\rho_i = \rho(\theta_i, \phi_i)$ will be denoted as (θ_{ia}, ϕ_{ia}) and (θ_{ib}, ϕ_{ib}) for the ρ_i matrices appearing in $\vec{a}'(u)$ and $\vec{b}'(v)$, respectively. It is important to note that the fact we can choose the angles at random means these are huge classes of independent solutions that we are free to analyze in order to obtain the statistics associated with the distribution of the cusps we are aiming for. By moving to the center-of-mass frame, we have induced an extra symmetry to the cosmic string loop, which now satisfies $\vec{X}(\tau, \sigma + \pi) = -\vec{X}(\tau, \sigma)$.

IV. CUSP OCCURRENCE

A generic property of cosmic strings is that points on the string can momentarily reach the speed of light. Differentiating Eq. (2.8) with respect to time, we find that

$$\dot{\vec{X}}(\tau, \sigma) = \frac{1}{2}(-\vec{a}'(u) + \vec{b}'(v)). \tag{4.1}$$

A point on the string reaches the speed of light when $|\dot{\vec{X}}|^2 = 1$, or equivalently when

$$\vec{a}'(u) = -\vec{b}'(v) \Leftrightarrow \vec{a}'(u) \cdot \vec{b}'(v) = -1. \tag{4.2}$$

The solutions of Eq. (4.2) are called cusps, and their location on the string worldsheet will be denoted as (u_c, v_c). Schematically, these solutions occur when $\vec{a}'(u)$ and $-\vec{b}'(v)$ intersect on the Kibble-Turok sphere (Fig. 1). Since the curves $\vec{a}'(u)$ and $\vec{b}'(v)$ are periodic, the cusp solutions (u_c, v_c) will also occur periodically. Smooth strings, arising from the Nambu-Goto action, will generically have cusp points. However, other types of strings can exist, with discontinuities in $\vec{a}'(u)$ and $\vec{b}'(v)$, called kinks. In this type of strings, cusps are more rare since the discontinuities make intersections on the Kibble-Turok sphere less likely to occur [2].

We wish to track down the occurrence of the cusps in our class of odd-harmonic strings. Unfortunately, it is clear that our key quantities (3.9) and (3.10) are nonlinear in u, v and Eq. (4.2) cannot be solved analytically in general. Hence, we will solve it numerically to obtain both the number of cusps formed per period, and by differentiating Eqs. (3.9) and (3.10) and evaluating them at (u_c, v_c), we will also obtain all the corresponding values for $\vec{a}''(u_c)$ and $\vec{b}''(v_c)$, respectively, another key quantity. Fortunately, there are in fact specific choices of parameters that do lead to analytic solutions for odd-harmonic strings. This is very useful as it will allow us to test our numerical algorithm, and so we now turn to these specific cases.

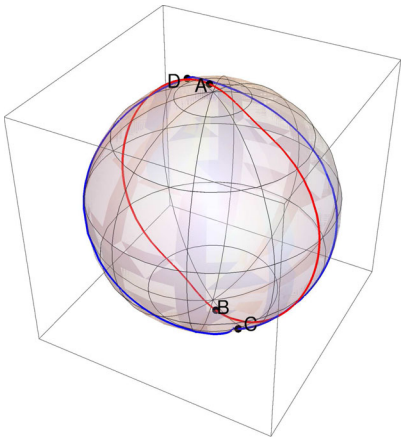

(a) The curves $\vec{a}'(u)$ (red) and $-\vec{b}'(v)$ (blue) on the sphere.

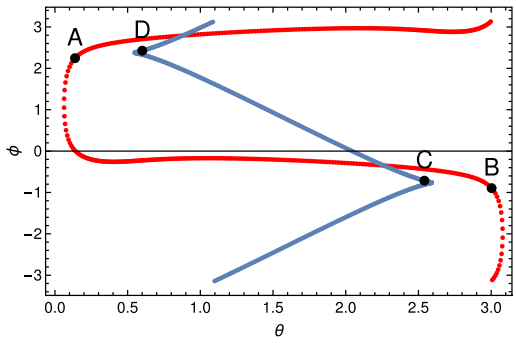

(b) The values of θ and ϕ as $\vec{a}'(\theta(u),\phi(u))$ and $-\vec{b}'(\theta(v),\phi(v))$ move on the sphere for N=3.

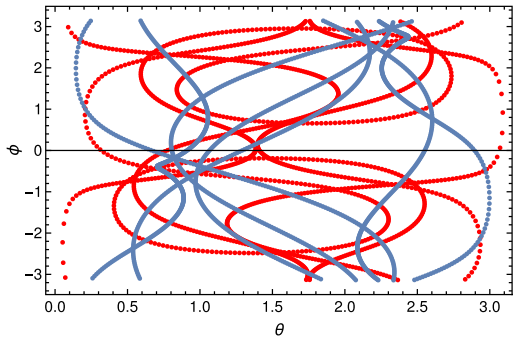

(c) The values of θ and ϕ as $\vec{a}'(\theta(u),\phi(u))$ and $-\vec{b}'(\theta(v),\phi(v))$ move on the sphere for N=13.

FIG. 1. Plots of the $\vec{a}'(u)$ and $\vec{b}'(v)$. In plots (a) and (b), we see the harmonic order $N=3$ case. The points depicted in the plots correspond to $A=(\theta_{\vec{a}'}(u=0),\phi_{\vec{a}'}(u=0))$, $B=(\theta_{\vec{a}'}(u=\pi),\phi_{\vec{a}'}(u=\pi))$, $C=(\theta_{\vec{b}'}(v=0),\phi_{\vec{b}'}(v=0))$, and $D=(\theta_{\vec{b}'}(v=\pi),\phi_{\vec{b}'}(v=\pi))$.

A. Analytic cases

An example of string solutions where the occurrence of cusps can be found analytically is the Kibble-Turok family of strings [44], which is a subset of the odd-harmonic string for certain choices of parameters in $\vec{a}_3'(u)$ and $\vec{b}_3'(v)$. They can be obtained from (3.9), (3.10) if we set $\theta_{3a}=0$, $\phi_{5a}=0$ and $\theta_{3b}=0$ and $\phi_{3b}=\pi$. The only free parameter is ϕ_{3a}, which we allow to range in the interval $[0,\pi]$. If we set $\alpha=\cos^2(\phi_{3a}/2)$, then the right- and left-movers are

$$\vec{a}'(u)=[(1-\alpha)\cos(u)+\alpha\cos(3u)]\vec{i} \tag{4.3}$$

$$+[(1-\alpha)\sin(u)+\alpha\sin(3u)]\vec{j} \tag{4.4}$$

$$+2\sqrt{\alpha(1-\alpha)}\sin(u)\vec{k} \tag{4.5}$$

and

$$\vec{b}'(v)=\cos(v)\vec{i}+\sin(v)\vec{j}. \tag{4.6}$$

The cusps positions can easily be obtained analytically for this family of loops by solving the cusp condition (4.2) for the above cosmic string solution, which provides a set of three equations with two unknowns. Note that the left-mover has no component in the z axis, which restricts the possible values of the u coordinate. The remaining two equations provide the possible v values and constrain the choices of pairs (u,v) that satisfy the system. We find that this family of string solutions supports two simultaneous cusps per period π at the points $(\tau,\sigma)=(\pi/2,\pi/2)$ and $(\tau,\sigma)=(\pi/2,3\pi/2)$.

Another analytic solution that can be described by our analysis is the first-order harmonic loop [64] obtained from (3.9) and (3.10) for $N=1$,

$$\vec{a}'(u)=\cos(u)\vec{i}+\cos\phi\sin(u)\vec{j}+\sin(\phi)\sin(u)\vec{k} \tag{4.7}$$

and

$$\vec{b}'(v) = \cos(v)\vec{i} + \sin(v)\vec{j}, \tag{4.8}$$

which also supports two cusps per period at $(\tau, \sigma) = (\pi/2, \pi/2)$ and $(\tau, \sigma) = (\pi/2, 3\pi/2)$. The cusp positions are found by solving the set of equations from (4.2), as we did for the Kibble-Turok string, by transforming from the coordinates (τ', σ') used in Ref. [64] to our coordinate system, via $\tau' = \tau$, $\sigma' = \sigma + \pi/2$ and $\phi' = \phi + \pi$. We were thus able to confirm the properties of both of these solutions with our numerical code, which we now go on to describe.

B. Numerical method

We will now summarize the structure of the code we used to solve the nonlinear system of equations (4.2). It consists of two parts, one to construct the loops and another to solve the nonlinear system. For simplicity, in what follows, we set the harmonic order of the left- and right-movers to be the same value N:

(1) Part I:
   (a) We choose the harmonic order N and the number of loops M (note that this is not the harmonic order of the left-movers M) we will analyze.
   (b) Adopting an iterative process, we produce the N-order harmonic loop in $(N-1)/2$ steps, using the definition of the odd-harmonic loop, Eqs. (3.9) and (3.10). In each step of the iteration, we randomly choose two angles for the $\vec{a}'_N(u)$ and two angles for $\vec{b}'_N(v)$, and in the last step, we randomly choose one extra angle for each of the left- and right-movers, which are needed to eventually build the N-harmonic loop with $2N-1$ random angles in total. In this way, we aim to sample the plane of angles, through a large number of random choices of angle parameters.
   (c) We append into lists the functions $\vec{a}'_N(u)$ and $\vec{b}'_N(v)$, their derivatives, $\vec{a}''_N(u)$ and $\vec{b}''_N(v)$, and the randomly chosen angles. The process of step 2 is repeated M times, to eventually obtain in lists all the required information for the M loops produced.

(2) Part II:
   (a) We enter an iterative process where we choose the ith element of the lists we have produced in part I, where i takes integer values from 1 to M, labeling the loop we are considering.
   (b) We divide the (u, v) plane into equally sized grids and numerically solve Eq. (4.2) to obtain the cusp solutions (u_c, v_c), which are then appended in a list and tested to check that they are indeed solutions, i.e., that they satisfy (4.2) by using the analytic expressions we saved from part I. We then increase the resolution of the grid by subdividing it into finer grid sizes and repeat the above process until no new (u_c, v_c) pairs are found. After we obtain the list of cusp points for the chosen loop, we calculate $|a''(u_c, v_c)|, |b''(u_c, v_c)|$.
   (c) This process is repeated until we analyze all loops from part I.

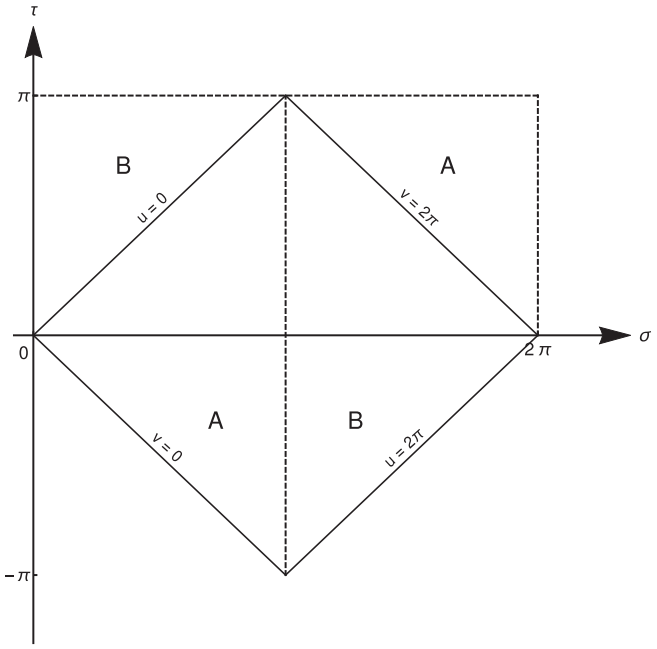

FIG. 2. The worldsheet domain in terms of the (τ, σ) and (u, v) coordinates.

Since the general equation of motion for the string comprises the periodic functions $\vec{a}(u)$ and $\vec{b}(v)$, each with a period 2π, the domain in $u - v$ space $[0, 2\pi) \times [0, 2\pi)$ contains all the information about the string motion. In Fig. 2, we can see that the $[0, 2\pi) \times [0, 2\pi)$ (u, v) domain can be mapped to the $[0, 2\pi) \times [0, 2\pi)$ (τ, σ) domain, as expected. Indeed, the domains labeled A in Fig. 2 are equivalent to each other, due to the periodicity of the string, $\vec{X}(\tau, \sigma) = \vec{X}(\tau + \pi, \sigma + \pi)$. The same holds for the domains B.

The numerical analysis of the strings can be quite time consuming. To reduce computational time, we take advantage of the extra symmetry of our string loop solutions in the center of mass frame, $\vec{X}(\tau, \sigma + \pi) = -\vec{X}(\tau, \sigma)$, which is equivalent to $\vec{X}(u, v) = \vec{X}(u + \pi, v + \pi)$. This implies that if a cusp occurs at (u_c, v_c), it also occurs at $(u_c + \pi, v_c + \pi)$, and we therefore only need to look for cusp solutions in the domain $[0, \pi) \times [0, 2\pi)$ of the $u - v$ space and then map them to the full domain $[0, 2\pi) \times [0, 2\pi)$ to obtain the full space of cusp solutions.

C. Results and discussion

To check on the accuracy of our simulations, we have compared our numerical results with the analytic cases mentioned in Sec. IV A, namely, the one-harmonic

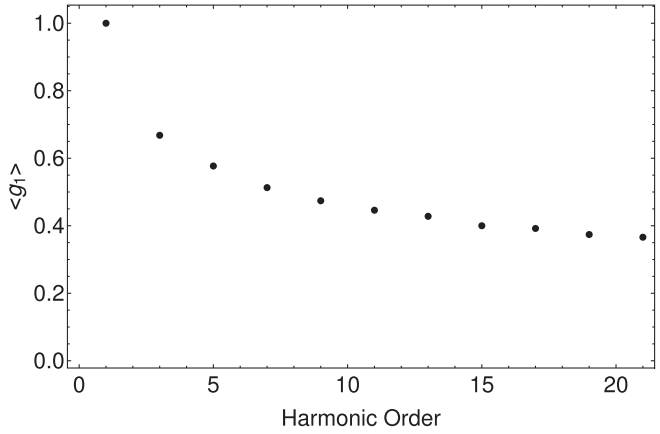

FIG. 3. Our numerical results for the mean value of g_1, with harmonic order from 1 to 21. Note that the harmonic order takes only odd values.

loop [64] and the Kibble-Turok loop [44], which can both be obtained from our odd-harmonic loops. In both cases, we find the same number and positions for the cusps, with an accuracy of 10^{-5}, and the same values for $|a_c''|$, $|b_c''|$ evaluated at the cusp. As a further check to our numerical method, we find that the Turok solution [66], a generalization of the Kibble-Turok string with two free parameters, exhibits (generically) either two or six cusps per period, with two of them always occurring at $(\tau, \sigma) = (\pi/2, \pi, 2)$ and $(\tau, \sigma) = (\pi/2, 3\pi, 2)$, as expected. Since the Turok string is not a subfamily of the odd-harmonic string, we input the equations of the left- and right-movers of the Turok string (given in Ref. [2]) directly into part II of our code (described in Sec. IV B). Note that the Turok string can also exhibit four cusps per period for a specific choice of its two free parameters. Since we choose these parameters randomly, it is unlikely that we will come across this fine-tuned case. The cusp structure of the Turok string with respect to the two-parameter space is provided in Ref. [64].

Having confirmed the consistency of our approach with known analytic solutions, we can confidently go on to look at cases of more general odd-harmonic strings, going up to harmonic order 21. The first question we wish to address is what is the average value of the second derivative of the left- and right-movers. Recall that this is an important contributor to the gravitational wave power emitted by cusps, and the assumption being made when calculating the associated gravitational wave power emerging from the cusp region is that in units of $2\pi/\ell$ the average value is of order 1 [27,50,52]. If it is substantially smaller, or if there are a significant number of cusps on a loop producing such small values, this will increase the associated power. Our key results are presented in Figs. 3 and 6. In Fig. 3, we have calculated the mean value for the second derivative of the left- and right-movers on the cusps defined through g_1, which was introduced in Ref. [52],

$$g_1 = (|\vec{a}''(u_c, v_c)||\vec{b}''(u_c, v_c)|)^{-\frac{1}{3}}, \tag{4.9}$$

for tens of thousands of loops as a function of the harmonic order, ranging from $N = 1$ to 21 [67]. This is so important because the gravitational wave amplitude is proportional to g_1. Of particular note is the fact that $\langle g_1 \rangle$ decreases rapidly initially as the harmonic order increases but eventually plateaus for large N. We also note that it is indeed consistent with the claims in Ref. [52], namely, that it is a number of order unity, given that it ranges from 1, for small N, down to 0.4, for large N.

What about the range of possible values of g_1 for a given harmonic? In particular, how large can it go, and how frequent are these large values? We address this question in Fig. 6, in which each of the four plots represents the frequency distribution of the parameter g_1 produced from a representative sample of 1000 loops of a specific harmonic order N. On the horizontal axis, we have the values of g_1, and on the vertical axis, we have the number of times the parameter g_1 obtains a value which lies in the corresponding bin. Note that the first plot, depicting the frequency distribution of g_1 for $N = 3$ harmonic loops, decreases almost monotonically from its initial high value in the [0.45, 0.5) bin, except for a secondary subsidiary peak in the [0.95, 1) bin. As we increase the number of harmonics N on the loop, the histograms become more peaked around small values of $g_1 \sim 0.4$, a feature that is particularly noticeable for the cases $N = 11$ and $N = 19$. We also notice that the total number of counts increases as we increase the harmonic order, N, of the loops. This occurs because the average number of cusps per period increases as we increase the harmonic order. We can understand the typical smallest value g_1 takes. For the case of the $N = 3$ harmonic order loop, we can show analytically [from Eqs. (3.9) and (3.10)] that it is 0.5, matching the numerical result. Unfortunately, analytic approaches break down for higher orders, as the function $g_1(u, v)$ quickly becomes complicated, and finding its maximum analytically becomes progressively harder. It is clear from the four cases depicted in Fig. 6 that the number of loops with large values of $g_1 \gg 1$ become negligible, and hence increasing the number of harmonics does not apparently have a significant impact in the range of possible values of g_1; they remain stubbornly close to the assumed value of order unity.

In Fig. 4, we plot the mean value of yet another quantity that is related to the gravitational wave signal emitted from cusps on cosmic strings. This is given by parameter g_2, defined in Ref. [52] as

$$g_2 = (\min(|\vec{a}''|, |\vec{b}''|))^{-1}, \tag{4.10}$$

which is inversely proportional to the beaming angle of the cusp θ^{div}. In particular, we define the angle θ^{div} to be the angle that divides the observation angles of a cusp into two

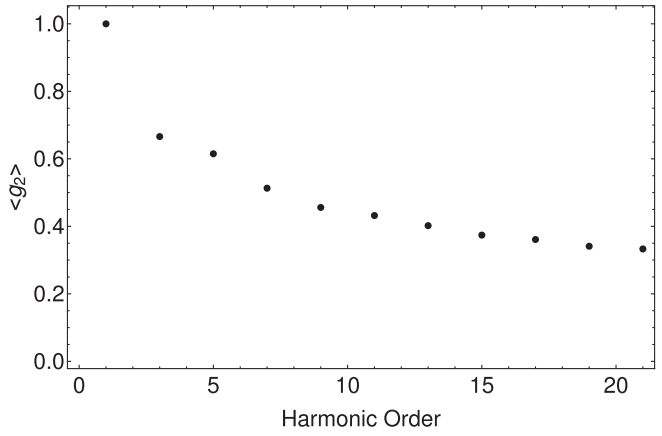

FIG. 4. Our numerical results for the mean value of g_2, with harmonic order from 1 to 21. Note that the harmonic order takes only odd values.

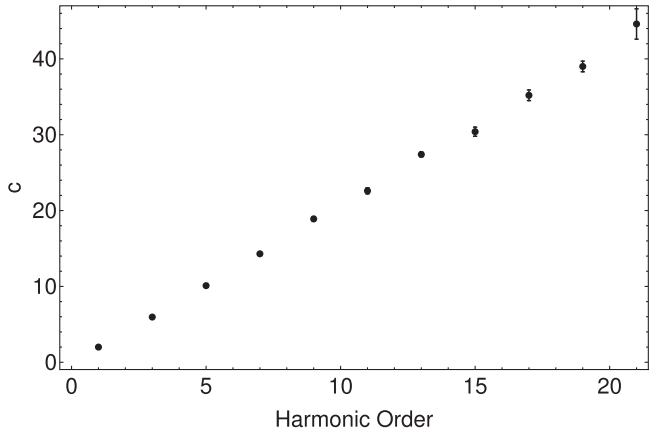

FIG. 5. Our numerical results for the mean value of the cusps per period c, with harmonic order from 1 to 21.

sets: one where the gravitational wave signal is roughly the same as it is along the direction of the cusp emission ($\theta < \theta^{\rm div}$) and one where the signal is smoothed ($\theta > \theta^{\rm div}$), which corresponds to the gravitational wave signal away from the cusp [51,52]. The observer receives the gravitational wave which has emanated from the cusp on the cosmic string if and only if the observation angle with respect to the direction of the cusp satisfies $\theta < \theta^{\rm div}$. As g_2 decreases, the angle $\theta^{\rm div}$ increases, which implies that the cusp signal can be received from a broader range of observation angles, and leads to an enhanced overall gravitational wave signal from cosmic strings on Earth. From Fig. 4, we notice that the average value of g_2 for each harmonic order follows a pattern similar to the one in Fig. 3, starting from an average value of unity at the first-order harmonic string and gradually decreasing in value until it plateaus at just below 0.4. Once again, we note that the values of g_2 obtained using the odd-harmonic string do not deviate significantly from the usual assumption that its value is equal to unity [51,52]. Given both g_1 and g_2 have basically the same dependence on $|\vec{a}''|$ and $|\vec{b}''|$, which typically have values of order unity, it is not surprising they have the same basic shape.

We believe that this result on the behavior of g_1 and g_2 can also be seen in the earlier very nice paper of Blanco-Pillado *et al.* [68], although it is not commented on directly there. Considering the shapes of loops resulting from including a smoothing process to model the effect of gravitational backreaction, they argue that smoothing leads to cusps of order 2 on each loop. In particular, in their Figs. 10 and 11, they plot the distribution over time of parameters which are closely related to g_1 and g_2, finding late time values for the two cusps, which remain on their loops that are very similar to the values we find here. Turning our attention to the number of cusps appearing per period on a harmonic order N string loop, c, we see from Fig. 5 the interesting result that the average value $\langle c \rangle$ shows a linear behavior (at least for N ranging from 1 to 21), satisfying $\langle c \rangle \simeq 2N$. We note that this result differs from that predicted in Ref. [54], in which it was suggested that $c \propto N^2$. The argument for N^2 is based on the fact that each mode roughly corresponds to a great circle on the Kibble-Turok sphere, so the number of intersections (i.e., the number of occasions a cusp forms) is proportional to N^2. It is not obvious to us at present why we are differing on this point; it is a very interesting question requiring further investigation. Figure 7 depicts the frequency distribution of the cusps per period produced from the class of 1000 loops represented in Fig. 6. It allows us to observe a general pattern of how the histogram changes with harmonic order. From the symmetries of the odd-harmonic string, we conclude that the number of cusps per period, c, has to be an even number. Also, note that in low harmonics it is far more likely to have values of c that are not multiplies of 4, as is clear from Fig. 7(a). This can be compared with the Turok solution [66], where c takes the value 4 only for very specific choices of the string parameters, and otherwise it takes the values 2 or 6 (see Ref. [64]). As the harmonic order increases, we notice that it becomes more likely to have values of c that are multiples of 4. It is worth noting a few interesting points from Figs. 5 and 7. First of all, note that, even for low harmonic loops with $N = 3$, there are on average six cusps per period, going up to approximately 40 for the case $N = 19$. For the 1000 $N = 3$ loops shown in Fig. 7, 650 of them have more than six cusps per period; for the $N = 5$ case, that number rises to 850; and for the $N = 19$ case, almost all the loops satisfy that condition. This raises the obvious question of what is the influence of these very cuspy loops when it comes to estimating the gravitational wave beaming from them. At the very least, it suggests that the effective number of cusps per period could well be significantly more than what has been assumed to date.

In Figs. 3–5, the error bars indicate the usual standard error associated with the mean. For Figs. 3 and 4, they turn

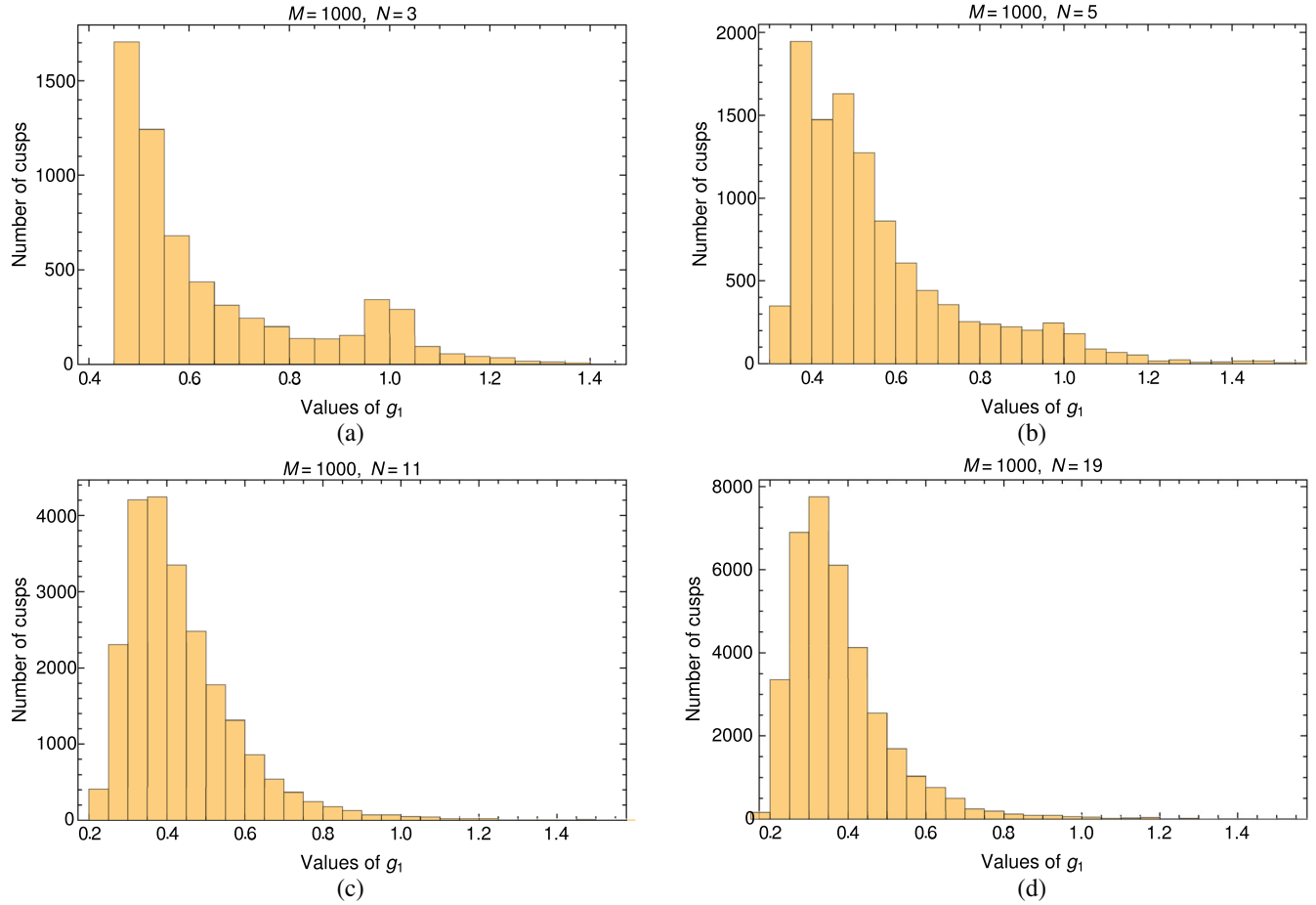

FIG. 6. The frequency distribution of the parameter g_1 calculated for different harmonic orders. Note that the data originate from a representative sample of $M = 1000$ cosmic string loops for each plot. We can see that the total number of cusps increases with the harmonic order, which is expected since the average number of cusps per period for each loop also increases with the harmonic order. Note that we have cut some rare higher values of g_1 from the histograms. The maximum value of g_1 in the data is given in Table.

out to be of order 10^{-4}, vanishingly small for all harmonic orders. However, in Fig. 5, the error bars increase for the highest harmonic loops we evolve because we are unable to analyze as many large harmonic loops due to the fact that such loops produce so many cusps per period, each of which need to be confirmed numerically. Note, however, that, although the number of high harmonic loops analyzed is smaller than for the low harmonic loops, the number of cusp events remains very large in all cases as cusps occur more often in every period for the high harmonic case. This explains that, while the error bars of the mean value of cusps per period with harmonic order, c, which appear in Fig. 5, become significant for harmonic orders 15 to 21, for the plots of g_1 and g_2 in Figs. 3 and 4, they remain small, even for the large harmonics.

Table I provides an elegant summary of our main results. In it, we show the values of the mean number of cusps per period for different harmonic order, as seen in Fig. 5. We also show the average values of g_1 and g_2 (including the maximum value we obtain for g_1) for each harmonic order. Finally, in Table I, we also show the size of the error bars in the value of c that appear in Fig. 5 for harmonic orders 15 to 21. The take home message is pretty clear; the "cusp sharpness" parameters g_1 and g_2 are fairly closely distributed around unity, as has been assumed in the literature, and we have now demonstrated this assumption is justified. In fact, if anything, they are slightly lower than unity, indicating the gravitational signals will be somewhat reduced from these effects (as far as g_1 is concerned), but mildly enhanced as far as g_2 is concerned, than has previously been assumed. On the other hand, as we discussed above, the average number of cusps per period, c, could be significantly enhanced for high-harmonic strings compared to the usual assumption $c \sim 1$. We will return to this point in Sec. V.

There is a nice formal mathematical aspect to the distribution of the (u_c, v_c) pairs on the plane. In Fig. 8, we can see that the pairs of harmonic order $N = 3$ follow a pattern, which does not persist for the higher harmonic orders, as we can see for the $N = 19$ case. We can quantify this using the two-dimensional Kolmogorov-Smirnov test, which shows that for large harmonic orders (we have tested

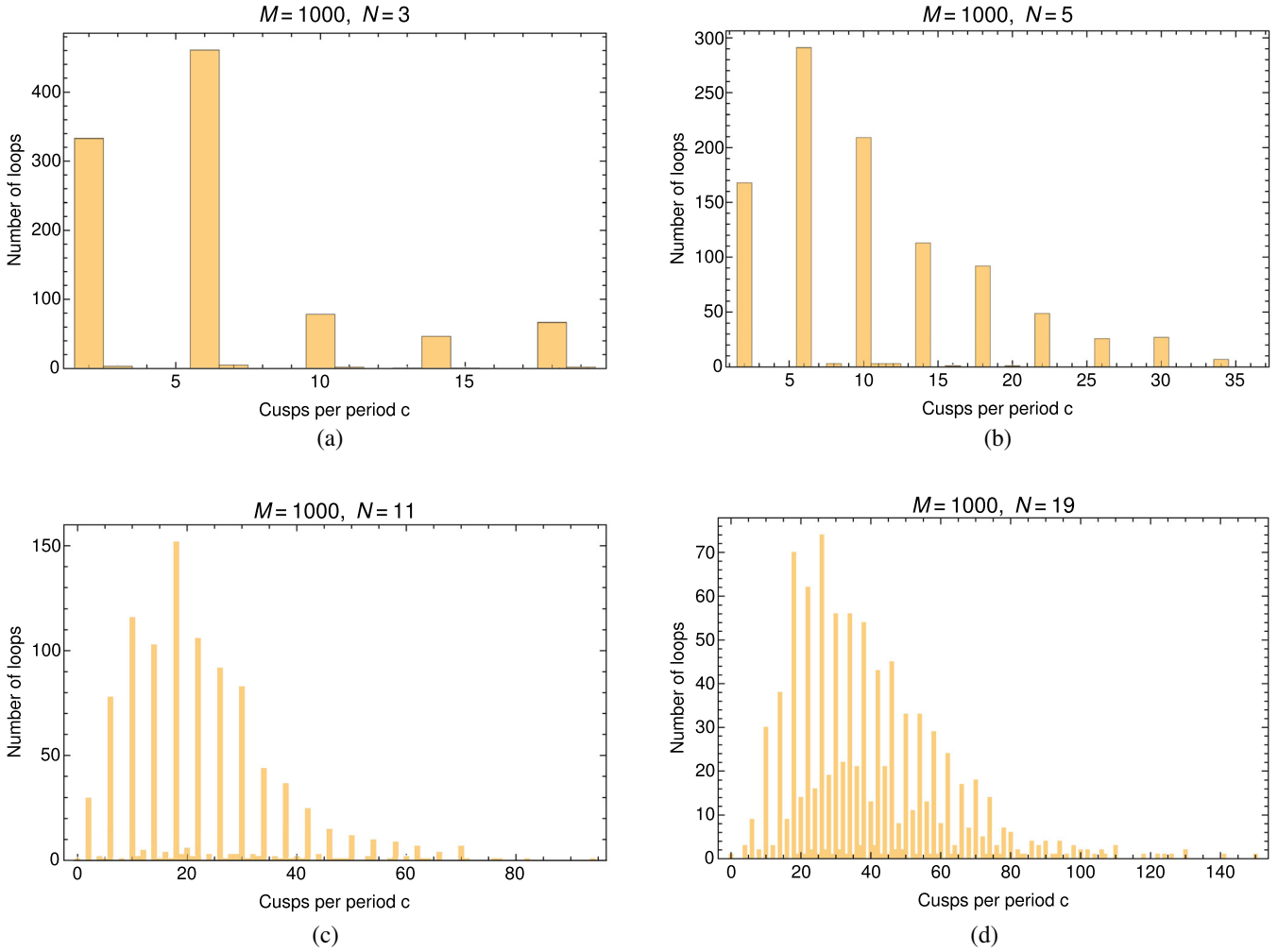

FIG. 7. The frequency distribution of the cusps per period. Each plot is produced from a representative sample of 1000 odd-harmonic string loops of the same harmonic order, $N = 3$, $N = 5$, $N = 11$, $N = 19$. The bins are $[0.5, 1.5), [1.5, 2.5), [2.5, 3.5), \ldots$.

TABLE I. Mean values of the cusp number per period and the average values of g_1 and g_2 evaluated at the cusp events for each harmonic order. We also provide the maximum value in the list of the values of g_1 we have obtained, $\{g_1\}$, for each harmonic order.

Harmonic order	c	$\langle g_1 \rangle$	Max$(\{g_1\})$	$\langle g_2 \rangle$
1	2.00	1.00	1.00	1.00
3	5.96	0.668	5.18	0.666
5	10.1	0.577	3.15	0.615
7	14.3	0.513	3.17	0.513
9	18.9	0.474	3.27	0.456
11	22.6	0.446	3.01	0.432
13	27.4	0.428	2.04	0.402
15	30.4 ± 0.6	0.400	3.35	0.374
17	35.2 ± 0.7	0.392	2.14	0.361
19	39.0 ± 0.7	0.375	1.91	0.341
21	44.6 ± 2.0	0.366	1.61	0.333

this up to $N = 19$) the hypothesis that the distribution of the (u_c, v_c) pairs follows the two-dimensional uniform distribution is not rejected at the 5% level (and so the distribution is consistent with being uniform). However, for harmonic order $N = 13$ and smaller, we find that the uniform distribution hypothesis is rejected at the 5% level, indicating there is some underlying structure present. Another way to test the behavior of the (u_c, v_c) pairs is to convert the two-dimensional distribution to a one-dimensional one. One way to achieve this is to split the domain $[0, 2\pi) \times [0, 2\pi)$ in $u - v$ space into equal sized squares. The number of the squares is taken to be of the order of the number of (u_c, v_c) pairs. We can then make a distribution of the number of (u_c, v_c) pair counts in each square and compare it with the Poisson distribution of the same mean value. Using the Kolmogorov-Smirnov test to compare these two distributions, we find again that the null hypothesis is rejected for $N = 13$ or smaller at the 5% level, while it is not rejected for $N = 15$ to $N = 19$, which is the maximum harmonic order we have tested.

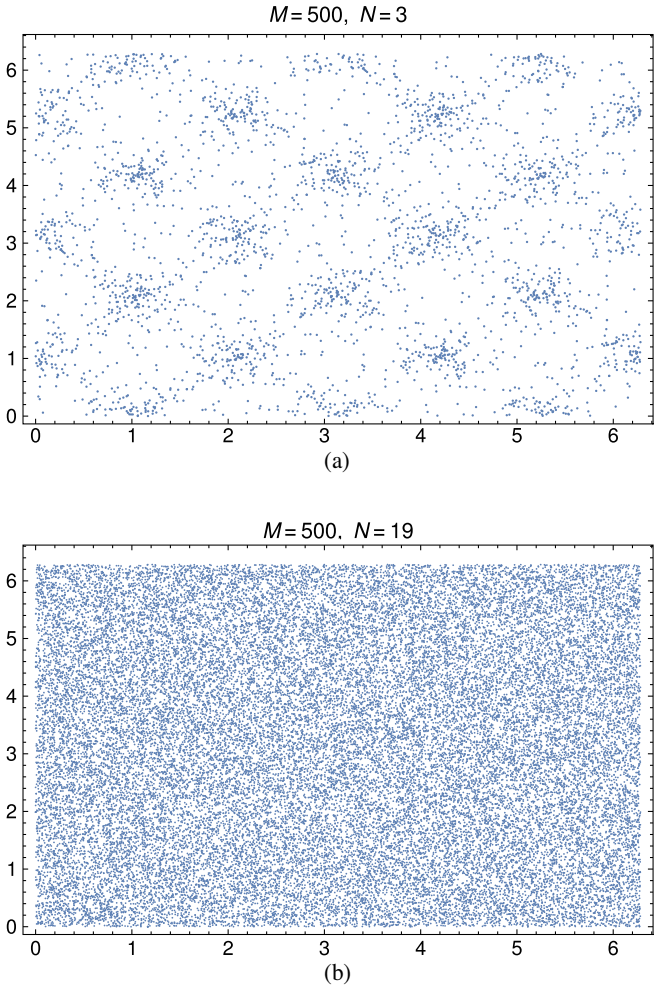

FIG. 8. The values of the (u_c, v_c) pairs on the u-v plane. Note that for $N = 3$ the pairs are more orderly placed, which is not observed for $N = 19$.

V. CONCLUSIONS

Cosmic strings have long been a favorite member of the particle cosmology family. Their formation out of symmetry breaking transitions in the early Universe placed them as excellent candidates to play a role in the physics of structure formation. However, as the data began to roll in, the evidence for such strings forming in a grand unified theory type transition failed to turn up; strings were not putting in an appearance in the cosmic microwave background anisotropies. It meant that interest in them waned, but that is not quite the same as the strings not being present or relevant. The breakthrough discovery of gravitational waves from the merger of a pair of black holes [69] has transformed the field and given hope to the possibility that cosmic strings may yet be detected by their emission of gravitational waves, either through the stochastic gravitational wave background or through bursts of gravitational waves emitted from cusps and kinks on a network [27,51,52]. Concentrating on three models for the loop production function, the lack of evidence of any signal of gravitational wave bursts from cusps and kinks associated with string loops allowed the authors of Ref. [27] to set upper limits on some of the key cosmic string parameters such as bounds on $G\mu$. However, in reaching those conclusions, they had to assume values for a number of key parameters, such as the average number of cusps formed per period on stable loop configurations, c (called N_q in Ref. [27]), and the average value of the product of the second derivatives of the left- and right-moving vectors on the loop evaluated at the cusp, to be precise g_1 and g_2 defined in Eqs. (4.9) and (4.10). These parameters which depend on the individual loops were both taken to be of order unity in Ref. [27] and associated papers, and yet the final result for the amplitude of the gravitational wave signal from the bursts depends on them. For example, if g_1 increases by a factor of 2, then the signal doubles.

It was this uncertainty in these key parameters that has motivated us to consider in this work the dynamics of cosmic string loops with higher harmonics. By going to higher harmonics, we can first of all compare the cusp distribution to those of lower harmonic loops, but crucially, we can gain excellent statistics on the range of values of $\vec{a}_N''$ and $\vec{b}_N''$, hence on the range of values of g_1 and g_2 associated with loops. Moreover, we have no way of *a priori* estimating the distribution of loops formed in the early Universe nor the distribution of the initial large parent loops chopped off a long string. In fact, it is quite likely they will be formed with many harmonics and begin oscillating with all of them in action. Given that, we have analyzed a class of such loops, albeit with odd harmonics, first demonstrated in the elegant work of Siemens and Kibble [65]. For simplicity, we concentrated on the case where the left- and right-moving waves on the loop had the same number of harmonics, and for each harmonic, we analyzed thousands of loops generated at random. This was done for all the odd harmonics up to $N = 21$. Two key results emerged. The first was that the average value for g_1 (and g_2) remained close to unity for all the harmonic cases studied, ranging from 1 (low harmonics) to 0.4 (high harmonics). In particular, there were very few cases where it went above unity, indicating that the assumptions made about its behavior (i.e., $g_1 \sim 1$, $g_2 \sim 1$) in Refs. [27,52] are correct. The second concerned the parameter c (N_q in Ref. [27]), the average number of cusps formed per period. Not surprisingly, we found that it grew with harmonic number N, but rather than growing as N^2 as argued for in Ref. [54], we found that it grew linearly obeying roughly $c = 2N$ as seen in Fig. 5 and Table I. One might expect that, because the amplitude of the gravitational wave burst signal from cusps appears to be proportional to c, such an increase in the average number of cusps per period would be an important feature, potentially leading to a significant enhancement of the gravitational wave signal from string loops due to cusps. However, it has recently been argued in

Ref. [70] that in at least one class of cosmic string loop models there is a cancellation of effects in that the larger number of cusps implies more radiation, but over a shorter period of time, and hence there is no net increase in the overall signal. Whether this cancellation happens in general for all models of cosmic string evolution remains to be seen, but it is certainly an important point showing that a careful comparison of these competing effects is necessary in any specific model of the loop network. There is also another caveat, and that is the bounds of Refs. [27,52] are based on the assumption that the loops being considered are non-self-intersecting. The loops we are studying here can be considered as the initial loops formed from the long string network that will no doubt self-intersect within the first oscillation. Such loops are constantly chopping off the network, and if there are a large number of cusps on these initial large loops, they may well modify the burst output in those opening oscillations compared to the loops which are assumed to have just one cusp per cycle. We have used the specific algorithm proposed by Kibble and Siemens [65] to obtain the shape of the class of loops we are analyzing. Although there is no question that these loops are valid solutions to the equations of motion, an argument against using them could be made based on the fact that they impose random phases, whereas loops that are found chopping off a network of strings and where cusps are introduced by gravitational backreaction [71] will have correlated phases. This is a fair criticism, but we believe our approach is a valid one. We have primarily been interested in the statistics of such cusps and their distributions, and this approach has allowed us to investigate tens of thousands of such cusps. Moreover, we find, where a comparison can be made, as mentioned earlier that the key parameters g_1 and g_2 appear to be consistent with those inferred in models of networks such as Ref. [68]. We will be addressing the impact of our loops on the gravitational wave signatures constrained by LIGO in a future publication [60] as well as modeling the process of self-intersection of these high harmonic initial loops.

ACKNOWLEDGMENTS

We would like to thank Dani Steer, Christophe Ringeval, Ken Olum, Jose Blanco-Pillado, Pierre Auclair, and Konstantinos Palapanidis for very useful conversations. Two of us (A. A. and E. J. C.) are very grateful to Ana Achucarro, Leandros Perivolaropoulos, Tanmay Vachaspati, and the Lorentz Center for organizing the workshop "Cosmic Topological Defects: Dynamics and Multi-messenger Signatures," where some of this work was discussed. A. A. and E. J. C. acknowledge support from STFC Grant No. ST/P000703/1. D. P. acknowledges support from the University of Nottingham Vice Chancellor's Scholarship.

[1] T. W. B. Kibble, Phys. Rep. **67**, 183 (1980).
[2] A. Vilenkin and E. P. S. Shellard, *Cosmic Strings and Other Topological Defects* (Cambridge University Press, Cambridge, England, 1994).
[3] M. B. Hindmarsh and T. W. B. Kibble, Rep. Prog. Phys. **58**, 477 (1995).
[4] M. Sakellariadou, Lect. Notes Phys. **718**, 247 (2007).
[5] E. J. Copeland and T. W. B. Kibble, Proc. R. Soc. A **466**, 623 (2010).
[6] E. J. Copeland, L. Pogosian, and T. Vachaspati, Classical Quant. Grav. **28**, 204009 (2011).
[7] W. Hu and M. J. White, Phys. Rev. D **56**, 596 (1997).
[8] U. L. Pen, U. Seljak, and N. Turok, Phys. Rev. Lett. **79**, 1611 (1997).
[9] A. Albrecht, R. A. Battye, and J. Robinson, Phys. Rev. Lett. **79**, 4736 (1997).
[10] A. Albrecht, R. A. Battye, and J. Robinson, Phys. Rev. D **59**, 023508 (1998).
[11] P. P. Avelino, E. P. S. Shellard, J. H. P. Wu, and B. Allen, Phys. Rev. Lett. **81**, 2008 (1998).
[12] P. A. R. Ade *et al.* (Planck Collaboration), Astron. Astrophys. **594**, A13 (2016).
[13] T. Charnock, A. Avgoustidis, E. J. Copeland, and A. Moss, Phys. Rev. D **93**, 123503 (2016).
[14] E. J. Copeland, A. R. Liddle, D. H. Lyth, E. D. Stewart, and D. Wands, Phys. Rev. D **49**, 6410 (1994).
[15] G. R. Dvali and S. H. H. Tye, Phys. Lett. B **450**, 72 (1999).
[16] C. P. Burgess, M. Majumdar, D. Nolte, F. Quevedo, G. Rajesh, and R. J. Zhang, J. High Energy Phys. 07 (2001) 047.
[17] N. T. Jones, H. Stoica, and S. H. H. Tye, Phys. Lett. B **563**, 6 (2003).
[18] R. Jeannerot, J. Rocher, and M. Sakellariadou, Phys. Rev. D **68**, 103514 (2003).
[19] C. P. Burgess, J. M. Cline, H. Stoica, and F. Quevedo, J. High Energy Phys. 09 (2004) 033.
[20] S. Kachru, R. Kallosh, A. D. Linde, J. M. Maldacena, L. P. McAllister, and S. P. Trivedi, J. Cosmol. Astropart. Phys. 10 (2003) 013.
[21] D. Baumann, A. Dymarsky, I. R. Klebanov, and L. McAllister, J. Cosmol. Astropart. Phys. 01 (2008) 024.
[22] M. Hindmarsh, J. Lizarraga, J. Urrestilla, D. Daverio, and M. Kunz, Phys. Rev. D **96**, 023525 (2017).
[23] D. Matsunami, L. Pogosian, A. Saurabh, and T. Vachaspati, Phys. Rev. Lett. **122**, 201301 (2019).
[24] P. Auclair, D. A. Steer, and T. Vachaspati, Phys. Rev. D **101**, 083511 (2020).

[25] B. P. Abbott *et al.* (LIGO Scientific Collaboration), Phys. Rev. D **80**, 062002 (2009).
[26] J. Aasi *et al.* (LIGO Scientific and VIRGO Collaborations), Phys. Rev. Lett. **112**, 131101 (2014).
[27] B. P. Abbott *et al.* (LIGO Scientific and Virgo Collaborations), Phys. Rev. D **97**, 102002 (2018).
[28] M. I. Cohen, C. Cutler, and M. Vallisneri, Classical Quant. Grav. **27**, 185012 (2010).
[29] P. Auclair *et al.*, J. Cosmol. Astropart. Phys. 04 (2020) 034.
[30] F. R. Bouchet and D. P. Bennett, Phys. Rev. D **41**, 720 (1990).
[31] M. S. Pshirkov and A. V. Tuntsov, Phys. Rev. D **81**, 083519 (2010).
[32] S. A. Sanidas, R. A. Battye, and B. W. Stappers, Phys. Rev. D **85**, 122003 (2012).
[33] C. Ringeval and T. Suyama, J. Cosmol. Astropart. Phys. 12 (2017) 027.
[34] J. J. Blanco-Pillado, K. D. Olum, and X. Siemens, Phys. Lett. B **778**, 392 (2018).
[35] C. J. A. P. Martins and E. P. S. Shellard, Phys. Rev. D **73**, 043515 (2006).
[36] C. Ringeval, M. Sakellariadou, and F. Bouchet, J. Cosmol. Astropart. Phys. 02 (2007) 023.
[37] V. Vanchurin, K. D. Olum, and A. Vilenkin, Phys. Rev. D **74**, 063527 (2006).
[38] F. Dubath, J. Polchinski, and J. V. Rocha, Phys. Rev. D **77**, 123528 (2008).
[39] M. Hindmarsh, S. Stuckey, and N. Bevis, Phys. Rev. D **79**, 123504 (2009).
[40] J. J. Blanco-Pillado, K. D. Olum, and J. M. Wachter, Phys. Rev. D **100**, 123526 (2019).
[41] J. J. Blanco-Pillado and K. D. Olum, Phys. Rev. D **96**, 104046 (2017).
[42] J. J. Blanco-Pillado, K. D. Olum, and B. Shlaer, Phys. Rev. D **89**, 023512 (2014).
[43] P. Auclair, C. Ringeval, M. Sakellariadou, and D. Steer, J. Cosmol. Astropart. Phys. 06 (**2019**) 015.
[44] T. W. B. Kibble and N. Turok, Phys. Lett. **116B**, 141 (1982).
[45] C. J. Burden, Phys. Lett. **164B**, 277 (1985).
[46] E. J. Copeland and N. Turok, Phys. Lett. B **173**, 129 (1986).
[47] J. J. Blanco-Pillado, K. D. Olum, and J. M. Wachter, Phys. Rev. D **100**, 023535 (2019).
[48] J. M. Wachter and K. D. Olum, Phys. Rev. Lett. **118**, 051301 (2017); **121**, 149901(E) (2018).
[49] M. J. Stott, T. Elghozi, and M. Sakellariadou, Phys. Rev. D **96**, 023533 (2017).
[50] D. Garfinkle and T. Vachaspati, Phys. Rev. D **36**, 2229 (1987).
[51] T. Damour and A. Vilenkin, Phys. Rev. D **71**, 063510 (2005).
[52] T. Damour and A. Vilenkin, Phys. Rev. D **64**, 064008 (2001).
[53] T. Damour and A. Vilenkin, Phys. Rev. Lett. **85**, 3761 (2000).
[54] C. J. Copi and T. Vachaspati, Phys. Rev. D **83**, 023529 (2011).
[55] R. J. Scherrer and W. H. Press, Phys. Rev. D **39**, 371 (1989).
[56] A. Albrecht and T. York, Phys. Rev. D **38**, 2958 (1988).
[57] T. York, Phys. Rev. D **40**, 277 (1989).
[58] R. J. Scherrer, J. M. Quashnock, D. N. Spergel, and W. H. Press, Phys. Rev. D **42**, 1908 (1990).
[59] P. Casper and B. Allen, Phys. Rev. D **52**, 4337 (1995).
[60] D. Pazouli, A. Avgoustidis, E. J. Copeland, and K. Palapanidis (to be published).
[61] D. B. DeLaney and R. W. Brown, Phys. Rev. Lett. **63**, 474 (1989).
[62] R. W. Brown, E. M. Rains, and C. C. Taylor, Classical Quant. Grav. **8**, 1245 (1991).
[63] B. Zwiebach, in *A First Course in String Theory* (Cambridge University Press, Cambridge, England, 2009), p. 673.
[64] M. R. Anderson, in *The Mathematical Theory of Cosmic Strings: Cosmic Strings in the Wire Approximation* (Institute of Physics, Bristol, England, 2003), p. 380.
[65] X. A. Siemens and T. W. B. Kibble, Nucl. Phys. **B438**, 307 (1995).
[66] N. Turok, Nucl. Phys. **B242**, 520 (1984).
[67] We should mention that it is much quicker to numerically evolve low harmonic loops than those with high harmonics because the latter possess far more cusps per period, each of which needs to be confirmed numerically—a time consuming process. As a result, we are able to analyze tens of thousands of loops with low harmonic numbers $N = 3, 5, \ldots$ but only 30 loops with $N = 21$. However, the total number of cusps formed remains large, even for the high harmonic loops.
[68] J. J. Blanco-Pillado, K. D. Olum, and B. Shlaer, Phys. Rev. D **92**, 063528 (2015).
[69] B. P. Abbott *et al.* (LIGO Scientific and Virgo Collaborations), Phys. Rev. Lett. **116**, 061102 (2016).
[70] P. G. Auclair, J. Cosmol. Astropart. Phys. 11 (2020) 050.
[71] We are very grateful to Jose Blanco-Pillado and Ken Olum for raising this point.